

of which were confirmed in the next generation. All 70 lines were backcrossed to wild-type plants, and at least 60 F₂ plants obtained by selfing of the F₁ progeny were scored for reselectability of the mutant phenotype to eliminate lines where the altered cell wall composition was caused by the combined action of several mutations.

6. L. Faye, K. D. Johnson, A. Sturm, M. J. Chrispeels, *Plant Physiol.* **75**, 309 (1989).
7. Purified cell wall material from *Arabidopsis* leaves was evenly suspended at a concentration of 2 mg/ml in 1 M H₂SO₄ containing *myo*-inositol (200 µg/ml) as an internal standard. This suspension was divided into six identical portions of 250 µl each, and three of these samples were spiked by addition of 5 µg of L-fucose each. The fucose content of the walls was calculated after gas chromatographic separation of alditol acetates (4), using the spiked samples as a reference. The amount of cell wall-derived fucose in the samples was 2.33 ± 0.25 µg.
8. Out of 167 F₂ plants, 128 were phenotypically wild type and 39 phenotypically mutant; $\chi^2 = 0.17$, $P > 0.6$.
9. Backcrossing to wild-type plants followed by the reselection of the mutant phenotype from segregating populations serves to reduce the number of background mutations.
10. The amount of residual fucose in leaves from pot-grown *mur1-2* plants was 1.0 ± 0.6% of the wild-type amount (sample size of 10); plants grown axenically on plates showed an approximately fourfold higher amount of residual fucose.
11. Gas chromatographic quantitation of L-fucose released from the sugar nucleotide fraction of leaf material indicated approximately 25-fold less L-fucose in the mutant than in the wild type, corroborating the conclusion that the *mur1* mutation affects the de novo synthesis of L-fucose.
12. Because the *mur1-1* and *mur1-2* lines were derived from independent mutagenesis events, they should differ in the location of background mutations, essentially eliminating the possibility that the visible phenotypes observed in both mutant lines were due to a mutation distinct from the *mur1* locus.
13. M. Estelle and C. R. Somerville, *Mol. Gen. Genet.* **206**, 200 (1987).
14. M. Koorneef and J. H. van der Veen, *Theor. Appl. Genet.* **58**, 257 (1980).
15. A. von Schaeuwen, A. Sturm, J. O'Neill, M. J. Chrispeels, *Plant Physiol.*, in press.
16. Inflorescences were harvested from plants in their middle flowering stages and prepared for measurements of tensile properties as follows: The whole apex of the inflorescence including the oldest mature flower was fixed between two layers of adhesive tape, then the lower part of the inflorescence was similarly taped, leaving a 4.5-mm segment of free stem between attachments. Flowers within this region were removed with fine scissors, and the tapes were cut to final sizes of about 3 by 3 mm each. Care was taken to avoid mechanical stress or damage to the stem segments during these steps. The taped segments were immediately frozen in liquid nitrogen and stored at -80°C. Breaking force measurements were carried out with the use of a custom-built extensometer as described by R. Prat and G. Parésy [*Plant Physiol. Biochem.* **27**, 955 (1989)]. The taped segments were thawed at room temperature for 2 min and inserted between the clamps of the extensometer (distance between clamps, 5.6 mm). The force exerted by the clamps was on the taped regions of the stems only, avoiding damage to the non-taped portion of the segments. The clamped segments were submerged in deionized water and extended at a rate of 2 mm/min until broken. Breakage occurred at the ends or in central parts of the segments with similar frequencies. A load-extension curve was recorded and evaluated for the force and energy required to break each segment. Breaking forces were usually in the 0.1 to 0.15 N range for segments from *mur1* plants and 0.25 to 0.35 N for segments from wild-type plants. To correct for differences in wall areas between individual plants, we cut the broken segments at their taped ends and

quantified the amount of cell wall material including cellulose (27) by gas chromatography of alditol acetates as described (4). The sum of the amounts of the cell wall-derived monosaccharides arabinose, xylose, galactose, and glucose were used for this normalization procedure.

17. D. M. Updegraff, *Anal. Biochem.* **32**, 420 (1969).
18. A. B. Blakeney, P. J. Harris, R. J. Henry, B. A. Stone, *Carbohydr. Res.* **113**, 291 (1983).
19. A. G. Darvill, M. McNeil, P. Albersheim, *Plant Physiol.* **62**, 418 (1978); T. T. Stevenson, A. G. Darvill, P. Albersheim, *Carbohydr. Res.* **182**, 207 (1988).
20. T. Hayashi and G. Maclachlan, *Plant Physiol.* **75**, 596 (1984); T. Hayashi, *Annu. Rev. Plant Physiol. Plant Mol. Biol.* **40**, 139 (1989); S. C. Fry, *J. Exp. Bot.* **40**, 1 (1989).
21. G. J. McDougall and S. C. Fry, *Plant Physiol.* **93**, 1042 (1990).
22. R. C. Smith and S. C. Fry, *Biochem. J.* **279**, 529 (1991); S. C. Fry *et al.*, *ibid.* **282**, 821 (1992).
23. S. Levy, W. S. York, R. Stuike-Prill, B. Meyer, L. A. Staehelin, *Plant J.* **1**, 195 (1991).
24. W. S. York, A. G. Darvill, P. Albersheim, *Plant*

Physiol. **75**, 295 (1984); G. J. McDougall and S. C. Fry, *Planta* **175**, 412 (1988); C. Augur *et al.*, *Plant Physiol.* **99**, 180 (1992).

25. G. J. McDougall and S. C. Fry, *Plant Physiol.* **89**, 883 (1989).
26. G. W. Haughn and C. R. Somerville, *Mol. Gen. Genet.* **204**, 430 (1986).
27. G. A. Adams, in *Methods in Carbohydrate Chemistry*, R. L. Whistler, Ed. (Academic Press, New York, 1965), vol. 5, pp. 269-275.
28. Plates contained 0.7% agar, 1% sucrose, and the basal salt mixture described by T. Murashige and F. Skoog [*Physiol. Plant.* **15**, 473 (1962)].
29. We thank M. Chrispeels for the *cgl* mutant. Supported by grants from the U.S. Department of Agriculture (91-37304) and the Department of Energy (DE-FG02-90ER20021), by a fellowship of the Natural Sciences and Engineering Research Council of Canada (to E.C.), and by fellowships of the Max Planck Society and the Deutsche Forschungsgemeinschaft (to W.-D.R.).

6 April 1993; accepted 9 June 1993

Group II Intron RNA Catalysis of Progressive Nucleotide Insertion: A Model for RNA Editing

Manfred W. Mueller,* Martin Hetzer, Rudolf J. Schweyen

The self-splicing *bl1* intron lariat from mitochondria of *Saccharomyces cerevisiae* catalyzed the insertion of nucleotidyl monomers derived from the 3' end of a donor RNA into an acceptor RNA in a 3' to 5' direction in vitro. In this catalyzed reaction, the site specificity provided by intermolecular base pair interactions, the formation of chimeric intermediates, the polarity of the nucleotidyl insertion, and its reversibility all resemble such properties in previously proposed models of RNA editing in kinetoplastid mitochondria. These results suggest that RNA editing occurs by way of a concerted, two-step transesterification mechanism and that RNA splicing and RNA editing might be prebiotically related mechanisms; possibly, both evolved from a primordial demand for self-replication.

The discovery of RNA molecules with enzymatic activities (ribozymes) and the diversity of the reactions that they catalyze have provoked interest in theories that suggest that early replicating systems were probably made of RNA or an RNA-like derivative (1-3). Zaug and Cech (4) demonstrated that RNA polymerization in a classical 5' to 3' polarity could be catalyzed by the self-splicing group I *Tetrahymena* intron. A pentamer of cytidylic acid (C₅) is converted to cytidylic acids up to C₃₀ by cleavage-ligation reactions (transesterification). The specificity for polycytidylic acids relies on base pair interactions with the intron internal guide sequence (IGS). A parallel between the function of the IGS sequence in RNA splicing and the proposed role for the guide RNAs (gRNAs) in RNA editing in kinetoplastid mitochondria (5-11) has been recognized (12, 13).

Theoretical considerations (13) and experimental evidence (12) suggest that post-

transcriptional uridine insertion and deletion occur by a series of splicing-like transesterification reactions (12, 13). The postulated chimeric intermediate with the gRNA covalently joined to the 3' portion of the mRNA (12) has been identified in vitro (14, 15). Although formation of the gRNA-mRNA chimeric intermediate can also be explained by separate cleavage and ligation reactions (16), other findings (14, 15) support the concerted transesterification model for uridine insertion in a 3' to 5' direction (12, 13) and suggest an evolutionary analogy to the catalytic mechanisms involved in RNA splicing (13).

Like group I self-splicing, self-splicing of the mitochondrial *Saccharomyces* group II intron *bl1* occurs by a two-step transesterification mechanism (17-19). The excised lariat intervening sequence (IVS) RNA acts as a ribozyme by catalyzing transesterification reactions with multiple turnover on ligated-exon RNA substrates in trans (20-23). This general recombinase and 3' terminal transferase activity of the group II lariat IVS is illustrated in Fig. 1A. Selection of the donor and acceptor RNA, and thereby specification of the transesterified

Vienna Biocenter, Institute for Microbiology and Genetics, University of Vienna, Dr. Bohr-Gasse 9, A 1030 Vienna, Austria.

*To whom correspondence should be addressed.

phosphorus atom in this charging-discharging pathway (20), is provided by intermolecular base pair interactions (EBS-IBS interaction) (24). The selection involves a minimum of six nucleotides in the substrate (IBS1: 5'-GACAGA) that are complementary to an intron internal guide sequence, the EBS1 site (5'-UCUGUC). This base pairing interaction renders the phosphorus atom 3' adjacent to the GACAGA motif (GACAGA:pN) in the donor RNA prone to a nucleophilic attack by the 3' oxygen atom of the lariat IVS (intron charging by transesterification). In a similar manner, in the discharging reaction the phosphorus atom that forms the 3' splice site becomes specifically transesterified by the 3' oxygen atom of the GACAGA sequence of the acceptor RNA (20).

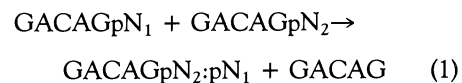
The *bII* lariat RNA can also catalyze an alternative form of IVS charging (20) when the phosphorus atom 5' adjacent to the canonical splice site becomes transesterified by the 3' oxygen atom of the lariat IVS [(-1) charging]. As a result, the IBS1 GACAGpA sequence of the donor RNA is dissected and the 3' terminal adenosine residue, together with the 3' exon portion, is transferred to the 3' end of the lariat IVS (20). Interacting cycles of IVS (-1) charging combined with accurate discharging by a GACAGA molecule may enable the *bII* lariat to act as a progressive RNA polymerase (nucleotidyl insertase) in an orderly 3'

to 5' direction in the manner illustrated (Fig. 1B, left).

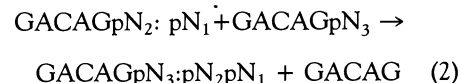
In the first step toward RNA polymerization, we synthesized an oligoribonucleotide (19-mer) that terminated in the GACAGA IBS1 sequence and assayed it in the presence of *bII* lariat RNA. The input molecules, labeled on their 5' ends with ^{32}P ($^*\text{pN}_{13}\text{GACAGpA}_1$; 19-mer), were progressively converted to products one nucleotide shorter at their 3' end (18-mer: $^*\text{pN}_{13}\text{GACAG}$) and to products elongated by one or more adenosines in length (for example, 25-mer: $^*\text{pN}_{13}\text{GACAGpA}_7$; $\text{pA}_6\text{pA}_5\text{pA}_4\text{pA}_3\text{pA}_2\text{pA}_1$) (Fig. 2A) (25). From these data, we predicted that the $^*\text{pN}_{13}\text{GACAGpA}$ input RNA is bifunctional in the reaction system and serves as the adenylyl-donating molecule in the charging reaction and as the adenylyl-accepting RNA in the discharging reaction (Fig. 1B). Because any activated nucleotidyl derivative should be polymerized by the lariat ribozyme, we examined the effect of varying the 3' terminal nucleotide of the natural IBS1 sequence ($^*\text{pN}_{13}\text{GACAGpA}$) (Fig. 2B). Among all four possible variants, $^*\text{pN}_{13}\text{GACAGpA}$ (Fig. 2A) and, to a lesser extent, $^*\text{pN}_{13}\text{GACAGpU}$ were converted to products one nucleotide shorter ($^*\text{pN}_{13}\text{GACAG}$) and with a longer chain length than the starting material. The variants $^*\text{pN}_{13}\text{GACAGpG}$ and $^*\text{pN}_{13}\text{GACAGpC}$ were

processed in the same way, although at a reduced efficiency (Fig. 2B).

The overall reaction is disproportional in the stoichiometry of the products and conservative in the total number of phosphodiester bonds in the system. The reaction can be formulated



Because the *bII* lariat IVS is regenerated in the reaction, it is expected to undergo multiple cycles of alternative charging combined with accurate discharging. When the $\text{GACAGpN}_2:\text{pN}_1$ product of reaction 1 is selected and serves as a substrate in a second round of (-1) charging, the disproportionation starts again:



The polarity of the RNA-catalyzed nucleotidyl insertion in the 3' to 5' direction was confirmed by experiments with the lariat intron (ribozyme) and two exogenous substrate RNAs (Fig. 3, A and B). An unlabeled 19-mer ($\text{N}_{13}\text{GACAGA}$) that terminated in the IBS1 sequence was co-assayed with a ^{32}P -labeled ligated exon RNA (36-mer; $\text{N}_{29}\text{GACAGA}:\text{pCp}$) that was provided with both IBS sequences (IBS1 and IBS2) of the natural 5' exon. The authentic

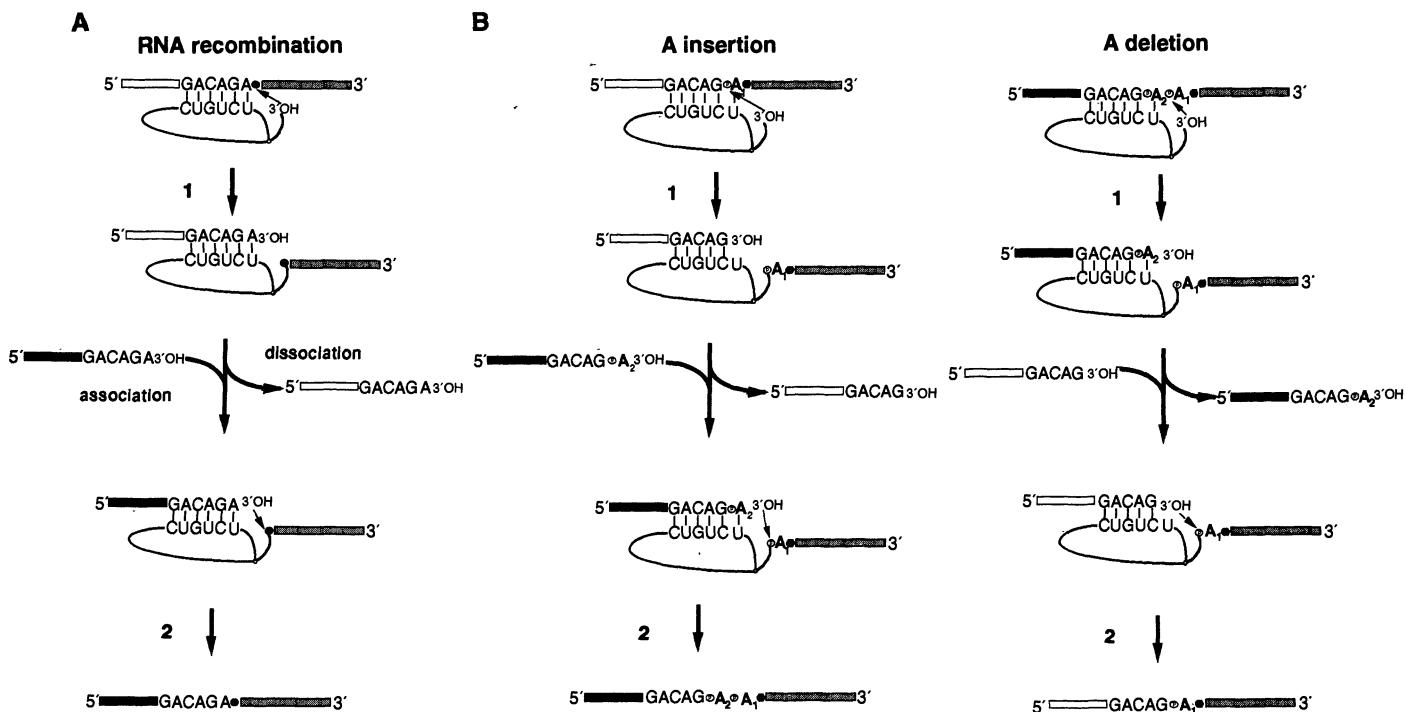


Fig. 1. Schematic representation of intermolecular transesterifications catalyzed by group II lariat RNA. Base pairing interactions of the IBS1 sequences (5'-GACAGA) with intronic EBS1 sequences (5'-UCUGUC) are indicated. Filled and open circles mark phosphodiester bonds involved in canonical and (-1) charging reactions, respectively. (A)

RNA recombination. In a two-step transesterification pathway that involves lariat IVS charging (1) and discharging (2), the 3' portion of a donor RNA becomes transferred to the 3' end of an acceptor molecule (20). (B) Predicted models for catalyzed adenosine insertion (left) and deletion (right) by two successive transesterifications.

3' exon was substituted with a *pCp mononucleotide that was labeled with ³²P specifically at the phosphorus atom that forms the ligation junction (20). The input ³²P radioactivity (36-mer) was progressively converted to oligoribonucleotidic acids with an electrophoretic mobility of a 20-mer (N₁₃-GACAGpA₁:*pCp) up to a 23-mer (N₁₃-GACAGpA₄:pA₃pA₂-pA₁*pCp) (Fig. 3A). The *pCp residue originating from the 3' end of the starting material (36-mer) formed the 3' terminal nucleotide of reaction products (26). When the elongated products were treated with ribonuclease U2, the ³²P radioactivity was totally converted to A*p. The ³²P-labeled phosphodiester bonds were formed between A-*pCp and consisted of normal 3'-5' phosphodiester linkages.

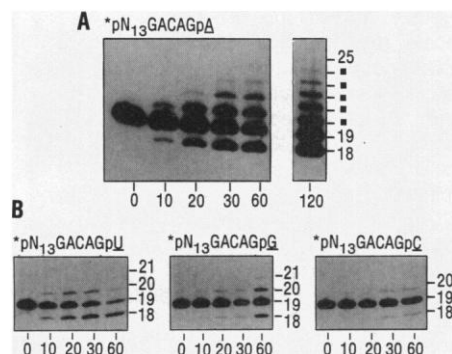


Fig. 2. Disproportionation of 5' end-labeled *pN₁₃GACAGpN RNAs (19-mer) in the presence of the *b11* lariat intron. Time (in minutes) is shown beneath each gel; numbers and squares at the side of gels indicate the respective length of fragments. **(A)** The *pN₁₃GACAGpA substrates (labeled on their 5' ends with ³²P) were incubated with lariat IVS as described (29). **(B)** Intron-catalyzed disproportionation of *pN₁₃GACAGpU, *pN₁₃GACAGpG, and *pN₁₃GACAGpC substrate RNAs, respectively.

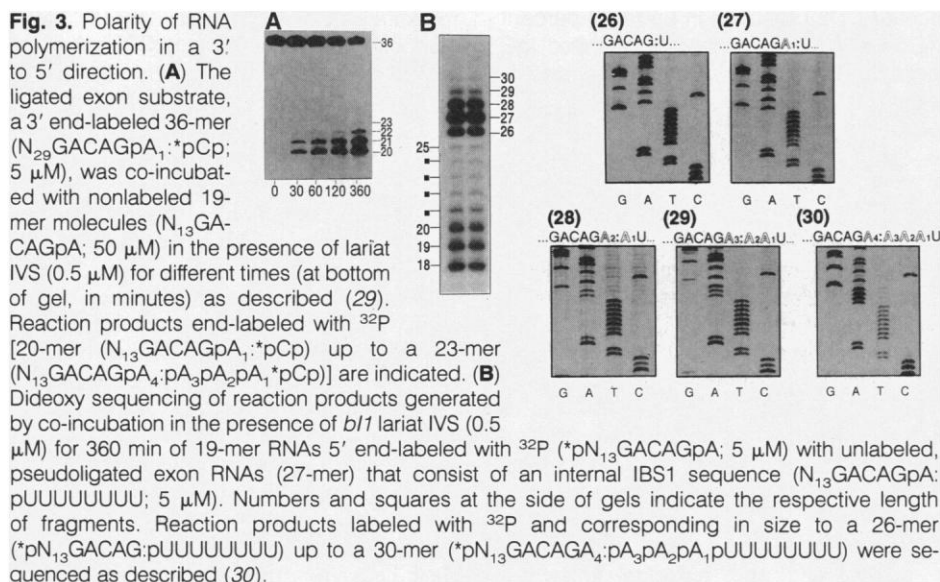


Fig. 3. Polarity of RNA polymerization in a 3' to 5' direction. **(A)** The ligated exon substrate, a 3' end-labeled 36-mer (N₂₉GACAGpA₁:*pCp; 5 μM), was co-incubated with nonlabeled 19-mer molecules (N₁₃GACAGpA; 50 μM) in the presence of lariat IVS (0.5 μM) for different times (at bottom of gel, in minutes) as described (29). Reaction products end-labeled with ³²P [20-mer (N₁₃GACAGpA₁:*pCp) up to a 23-mer (N₁₃GACAGpA₄:pA₃pA₂pA₁*pCp)] are indicated. **(B)** Dideoxy sequencing of reaction products generated by co-incubation in the presence of *b11* lariat IVS (0.5 μM) for 360 min of 19-mer RNAs 5' end-labeled with ³²P (*pN₁₃GACAGpA; 5 μM) with unlabeled, pseudoligated exon RNAs (27-mer) that consist of an internal IBS1 sequence (N₁₃GACAGpA:pUUUUUUUU; 5 μM). Numbers and squares at the side of gels indicate the respective length of fragments. Reaction products labeled with ³²P and corresponding in size to a 26-mer (*pN₁₃GACAG:pUUUUUUUU) up to a 30-mer (*pN₁₃GACAGpA₄:pA₃pA₂pA₁pUUUUUUUU) were sequenced as described (30).

A more direct confirmation of the predicted polarity was then performed. A 19-mer, labeled at its 5' end with ³²P and terminating in the GACAGpA IBS1 sequence, was co-incubated in the presence of *b11* lariat IVS with an unlabeled substrate that comprised an internal IBS1 sequence followed by a run of eight uridine residues (27-mer; N₁₃GACAGpA:pUUUUUUUU). The input ³²P radioactivity, originating from the 19-mer (*pN₁₃GACAGpA₁), was transferred to oligoribonucleotidic acids with an electrophoretic mobility of an 18-mer (*pN₁₃GACAG) up to a 25-mer (*pN₁₃GACAGpA₇:pA₆pA₅pA₄pA₃pA₂-pA₁). In addition, labeled reaction products elongated by the series of the U₈ pseudo 3' exon were obtained (Fig. 3B). The predicted identity of these products that corresponded in size to a 26-mer (*pN₁₃GACAG:pUUUUUUUU) up to a 30-mer (*pN₁₃GACAGpA₄:pA₃pA₂pA₁pUUUUUUUU) was determined by dideoxy sequencing (Fig. 3B). On the basis of these data, we suggest that the adenosine insertion catalyzed by the group II lariat IVS proceeds in a 3' to 5' direction. This polarity differs from modern protein RNA or DNA polymerases and from previously reported RNA-catalyzed polymerization reactions of the shortened versions of the *Tetrahymena* group I IVS (4, 27).

Because the lariat IVS-catalyzed RNA polymerization is conservative in the total number of O-P bonds that are broken and rejoined in the system, the reaction is expected to be highly reversible. If the 3' terminally processed 18-mer RNA (N₁₃GACAG) rebinds to a charged lariat IVS intermediate (IVS:pA₁*pCp or IVS:pA₁UUUUUUUU, respectively) and attacks the phosphodiester linkage that forms the 3' splice site, the original starting material (N₁₃GACAGpA₁:

*pCp or N₁₃GACAGpA₁:pUUUUUUUU) is regenerated. This is essentially the true reversion of reaction 1. Furthermore, accurate charging of the lariat IVS at the natural phosphodiester bond 3' adjacent to the GACAG sequence, followed by discharging by a processed GACAG product, is expected to compete with the extent of the adenylyl insertion by reversion of reaction 2 (Fig. 1B, right).

We have demonstrated an in vitro nucleotidyl insertion-deletion system catalyzed by the group II intron; this system could bridge the gap between catalytic strategies of RNA self-splicing (19) and recently proposed models of RNA editing in kinetoplastid mitochondria (12, 13). In contrast with canonical RNA editing in kinetoplastid protozoa (6-11), the guide sequence (EBS1) in the group II intron-catalyzed system is complementary to the 5' portion of the RNA fragment rather than to the 3' portion. Furthermore, the 5' RNA fragment, instead of the nonencoded 3' terminal oligo(U) tail (14, 15), provides the source of the transferred nucleotidyl derivative of the gRNA itself (12, 28). The site specificity provided by intermolecular base pairing interactions, chimeric intermediate formation, and the polarity of the insertion-deletion mechanism all support the idea that RNA splicing and RNA editing are evolutionarily related mechanisms (12, 13), both accomplished by a concerted, two-step transesterification mechanism (12-15).

It remains to be verified if, in group II-catalyzed nucleotidyl insertion-deletion as well as in RNA editing, the complement of the extension of the guide sequence (EBS1 and gRNA, respectively) will be synthesized by a trial and error process that discriminates between nucleotide insertion and deletion. The implications of this, especially in view of proposed early replicating systems made of RNA or an RNA-like derivative (1-3), merits further investigation.

REFERENCES AND NOTES

1. T. R. Cech, *Proc. Natl. Acad. Sci. U.S.A.* **83**, 4360 (1986).
2. J. A. Doudna and J. W. Szostak, *Nature* **339**, 519 (1989).
3. G. F. Joyce, *ibid.* **338**, 217 (1989).
4. A. J. Zaugg and T. R. Cech, *Science* **231**, 470 (1986).
5. L. Simpson and J. Shaw, *Cell* **57**, 355 (1989).
6. J. E. Feagin, *J. Biol. Chem.* **265**, 19373 (1990).
7. R. Benne, *Trends Genet.* **6**, 177 (1990).
8. C. Weissmann, R. Cattaneo, M. A. Billeter, *Nature* **343**, 697 (1990).
9. A. M. Weiner and N. Maizels, *Cell* **61**, 917 (1990).
10. K. Stuart, *Trends Biochem. Sci.* **16**, 68 (1991).
11. B. Sollner-Webb, *Nature* **356**, 743 (1992).
12. B. Blum, N. R. Sturm, A. M. Simpson, L. Simpson, *Cell* **65**, 543 (1991).
13. T. R. Cech, *ibid.* **64**, 667 (1991).
14. D. J. Koslowsky, H. U. Göringer, T. H. Morales, K. Stuart, *Nature* **356**, 807 (1992).
15. M. E. Harris and S. L. Hajduk, *Cell* **68**, 1091 (1992).

16. B. Sollner-Webb, *Curr. Opin. Cell Biol.* 3, 1056 (1991).
17. C. Schmelzer and R. J. Schweyen, *Cell* 46, 557 (1986).
18. C. Schmelzer and M. W. Müller, *ibid.* 51, 753 (1987).
19. T. R. Cech, *Science* 236, 1532 (1987).
20. M. W. Müller, P. Stocker, M. Hetzer, R. J. Schweyen, *J. Mol. Biol.* 222, 145 (1991).
21. M. Mörl and C. Schmelzer, *Nucleic Acids Res.* 18, 6545 (1990).
22. S. Augustin, M. W. Müller, R. J. Schweyen, *Nature* 343, 383 (1990).
23. M. Mörl and C. Schmelzer, *Cell* 60, 629 (1990).
24. A. Jacquier and F. Michel, *ibid.* 50, 17 (1987).
25. The identity of these products was confirmed by dideoxy sequencing with reverse transcriptase after 3' terminal tagging of the reaction products with a deoxyoligonucleotide in the presence of T4 RNA ligase.
26. Treatment of gel-purified reaction products with T4 polynucleotide kinase, which had 3' phosphatase activity at pH 5.0 [V. Cameron and O. C. Uhlenbeck, *Biochemistry* 16, 5120 (1977)], resulted in a slower electrophoretic mobility.
27. M. D. Been and T. R. Cech, *Science* 239, 1412 (1988).
28. R. J. Atkinson, W. A. Mathews, P. A. Newman, R. A. Plumb, *Nature* 340, 290 (1989).
29. Synthetic oligoribonucleotides (19-mer) [5'-GG-GAACAAAGGAAGACAG(N); where N is A, U, G, or C] were synthesized, labeled on the 5' end, and purified as described (20). The *b11* lariet IVS RNA was produced by RNA splicing in vitro as reported (20). Oligoribonucleotides (5 μ M) labeled on their 5' ends and *b11* lariet IVS (0.5 μ M) were incubated in 40 mM Tris, 60 mM MgCl₂, 2 mM spermidine, and 500 mM NH₄Cl (pH 7.5) at

45°C. Samples were taken from 0 to 120 min as indicated, analyzed, and quantified as described (20).

30. Synthetic oligoribonucleotides, containing IBS1 and IBS2 sequences (5'-GGGAACAAAGGTTAATTGT-TGTGTTTATGGACAGA; 35-mer) and pseudoligated substrate RNAs that comprised an internal IBS1 sequence (5'-GGGAACAAAGGAAGACAGA:pUUUUUUUU; 27-mer) were synthesized and purified as described (20). The sequence N₂₉-GACAGA:pCp was prepared as described (20). Labeled reaction products that corresponded in size to a 26-mer (*pN₁₃GACAG:pUUUUUUUU) up to a 30-mer (*pN₁₃GACAGpA₄pA₃pA₂pA₁pUUUUUUUU) were gel extracted and tagged by virtue of their 3' terminal OH group to the 5' phosphate group of the Eco RI site of plasmid BS/b11 (22) DNA in the presence T4 RNA ligase (20). The 3' OH group of the Eco RI site was used to initiate the complementary DNA (cDNA) synthesis of the covalently ligated RNA products. Amplification with the polymerase chain reaction was performed with a *b11* internal oligonucleotide (5'-GATTAATGTGAAAGCATGCTAACTTC, nucleotides 635 to 660 on the plus strand of *b11* and biotinylated on the 5' end) in conjunction with an oligonucleotide partially complementary to the 5' part of the cDNA sequence (5'-AAATCTGGTAACGGGAACAAAGGAAGAC). Direct solid-phase sequencing was performed as described [T. Hultman, S. Staahl, E. Hornes, M. Uhlen, *Nucleic Acids Res.* 17, 4937 (1989)].
31. We thank K. Tedin, J. Dittami, and A. von Gabain for critical review of the manuscript. Supported by the Austrian Ministry of Science and Research and the Austrian Fonds zur Förderung der wissenschaftlichen Forschung.

24 March 1993; accepted 14 June 1993

Inhibition of an in Vivo Antigen-Specific IgE Response by Antibodies to CD23

Leopoldo Flores-Romo, John Shields, Yves Humbert, Pierre Graber, Jean-Pierre Aubry, Jean-François Gauchat, Guidon Ayala, Bernard Allet, Marcela Chavez, Hervé Bazin, Monique Capron, Jean-Yves Bonnefoy*

Immunoglobulin E (IgE) mediates many allergic responses. CD23 is a 45-kilodalton type II transmembrane glycoprotein expressed in many cell types. It is a low-affinity IgE receptor and interacts specifically with CD21, thereby modulating IgE production by B lymphocytes in vitro. In an in vivo model of an allergen-specific IgE response, administration of a rabbit polyclonal antibody to recombinant human truncated CD23 resulted in up to 90 percent inhibition of ovalbumin-specific IgE synthesis. Both Fabs and intact IgG inhibited IgE production in vitro and in vivo. Thus, CD23 participates in the regulation of IgE synthesis in vivo and so could be important in allergic disease.

In vitro studies with some antibodies to CD23 (1, 2) or soluble CD23 fragments (3) have implicated this molecule in the regulation of IgE synthesis. To investigate the

L. Flores-Romo, J. Shields, Y. Humbert, P. Graber, J.-P. Aubry, J.-F. Gauchat, G. Ayala, B. Allet, J.-Y. Bonnefoy, Glaxo Institute for Molecular Biology, CP 674, CH-1228 Geneva, Switzerland.

M. Chavez and H. Bazin, Experimental Immunology Unit, University of Louvain, Faculty of Medicine, B-1200 Brussels, Belgium.

M. Capron, Centre d'Immunologie et de Biologie Parasitaire, INSERM U167-CNRS 624, Rue du Professeur Calmette, 59019 Lille, France.

*To whom correspondence should be addressed.

importance of CD23 in the production of IgE in vivo [CD23 is a low-affinity receptor for IgE (4)], we used a rabbit polyclonal antibody (Rb55) that was raised to a truncated form of the human CD23 molecule. The immunogen, a 25-kD form of CD23, corresponded to amino acids 150 to 321 of full-length CD23 (5) and was produced in *Escherichia coli*. It was purified from a washed pellet of *E. coli* by ion-exchange and gel filtration chromatography and has the expected NH₂-terminal sequence (6). This 25-kD CD23 antigen was injected into a rabbit, and the resulting antiserum

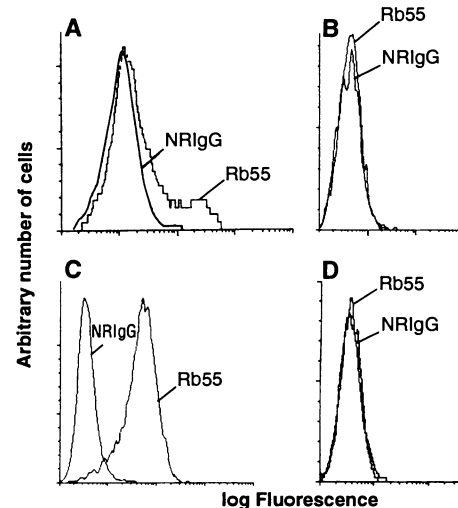


Fig. 1. The binding of Rb55 to a 45-kD molecule expressed on CD23-positive but not on CD23-negative cells. Flow cytometric analysis of (A) COS cells transfected with full-length human CD23 (5), (B) COS cells mock-transfected, (C) CD23-positive lymphoblastoid RPMI 8866 cell line, and (D) CD23-negative Burkitt lymphoma Daudi cell line. Cells were stained with affinity-purified Rb55 (7) or normal rabbit IgG (NRIgG) (both at 10 μ g/ml) and fluorescein isothiocyanate (FITC)-conjugated goat antibodies to rabbit IgG (1 μ g/ml) (Silenus, Victoria, Australia). Cells (5000) were analyzed on a FACScan (Becton Dickinson, Erembodegem, Belgium). (E) Protein immunoblot analysis of CD23-positive and -negative cells. Cell lysates were subjected to SDS-PAGE. We transferred the separated proteins to a nitrocellulose filter and blotted them with Rb55 and horseradish peroxidase (HRP)-labeled goat antibodies to rabbit IgG (Sigma, St. Louis, Missouri). The mass standards are indicated at the left in kilodaltons. Lane 1, mock-transfected COS cells; lane 2, Daudi cells; lane 3, CD23-transfected COS cells; and lane 4, RPMI 8866 cells.

(Rb55) (7) tested positive in both an enzyme-linked immunosorbent assay (ELISA) and protein immunoblot with purified recombinant human CD23. An IgG fraction, isolated by protein A-Sepharose affinity chromatography, recognized recombinant CD23 expressed on COS cells transfected with cDNA encoding the full-length molecule as well as native CD23, as expressed on the Epstein-Barr virus (EBV)-transformed lymphoblastoid cell line RPMI 8866. Both CD23s were 45 kD (Fig. 1). Affinity-purified Rb55 IgG molecules and Fabs of Rb55 (7) were found to inhibit interleukin-4 (IL-4)-induced IgE production by human mononuclear cells in vitro in an isotype-specific